J|A|C|S ARTICLES

Published on Web 07/20/2009

Microwave-Assisted Synthesis of Thiophene Fluorophores, Labeling and Multilabeling of Monoclonal Antibodies, and Long Lasting Staining of Fixed Cells

Massimo Zambianchi,[†] Francesca Di Maria,[†] Antonella Cazzato,[‡] Giuseppe Gigli,[§] Manuel Piacenza,[§] Fabio Della Sala,[§] and Giovanna Barbarella*,[†]

Consiglio Nazionale Ricerche CNR-ISOF and Mediteknology srl, Via Gobetti 101, 40129 Bologna, Italy, and National Nanotechnology Laboratory (NNL) of INFM-CNR and Dip. Ingegneria Innovazione, Università del Salento, Via Arnesano, 73100 Lecce, Italy

Received March 26, 2009; E-mail: barbarella@isof.cnr.it

Abstract: We report the expedient microwave-assisted synthesis of thiophene based 4-sulfo-2,3,5,6,-tetrafluorophenyl esters whose molecular structure was engineered to achieve blue to red bright fluorescence. The reactivity toward monoclonal antibodies of the newly synthesized fluorophores was analyzed in comparison with that of the corresponding *N*-succinimidyl esters. Single-fluorophore and multiple-fluorophore labeled antibodies were easily prepared with both types of esters. Multiple-fluorophore labeling with blue and orange emitting fluorophores resulted in white fluorescent antibodies. Thiophene based fluorophores displayed unprecedented fluorescence stability in immunostaining experiments. First-principles TD-DFT theoretical calculations helped us to interpret the behavior of fluorescence emission in different environments.

1. Introduction

Expanding the tool box of currently available fluorescent probes for the monitoring of biological systems and processes is a challenge crucial to several research areas spanning from medical diagnostics to genomics and live cell metabolism.[1] In the past few years understanding the molecular basis of diseases and developing new methods for genetic testing as well as environmental monitoring, security problems, and forensic analyses have become topics of central importance. In all these fields, new and more efficient analytical tools to characterize nucleic acids, proteins, and cells and the production of low cost, easy to manipulate systems for fast sample analysis and large-scale screening are highly required. In this rapidly developing context, fluorescent detection has become one the most exploited techniques owing to its sensitivity and noninvasiveness.[2] Unfortunately, a universal class of fluorophores applicable to all the fields of interest has not yet been described. There are many classes of fluorophores—molecular, macromolecular, dendrimeric, nanostructured, some of which already commercial—that are employed more or less efficiently in specific applications.[1]

One of the best classes of fluorophores described so far is that of Green Fluorescent Proteins (GFPs), worthy of the Chemistry Nobel Prize 2008.[3] GFPs are genetically encoded fluorescent tags; joining GFPs to a protein of interest allows the fluorescent imaging of the protein within the cell.[4] Variants of GFP are able to emit light in many different colors.[5] Fluorescent proteins are a great achievement, yet still other biomolecules not directly encoded by the genome such as nucleic acids, glycans, lipids, or secondary metabolites cannot be imaged by this method.

Another class of fluorescent probes that has enjoyed great attention in the past few years is that of quantum dots (QDs), nanocolloids made of CdSe or other inorganic nanocrystals.[6,1c] Different strategies of QD surface modification and coating

[†] Consiglio Nazionale Ricerche CNR-ISOF.
[‡] Mediteknology srl.
[§] Università del Salento.

(1) (a) Sameiro, M.; Gonçalves, T. *Chem. Rev.* **2009**, *109*, 190–212. (b) Lavis, L. D.; Raines, R. T. *ACS Chem. Biol.* **2008**, *3*, 142–155. (c) Mann, S. *Angew. Chem., Int. Ed.* **2008**, *47*, 2–17. (d) Resch-Ganger, U.; Grabolle, M.; Cavaliere-Jaricot, S.; Nitschke, R.; Nann, T. *Nat. Methods* **2008**, *5*, 763–775. (e) Chen, A. K.; Cheng, Z.; Behlke, M. A.; Tsourkas, A. *Anal. Chem.* **2008**, *80*, 7437–7444. (f) Simeonov, A.; Jadhav, A.; Thomas, C. J.; Wang, Y.; Huang, R.; Southall, N. T.; Shinn, P.; Smith, J.; Austin, C. P.; Auld, D. S.; Inglese, J. *J. Med. Chem.* **2008**, *51*, 2363–2371. (g) Longmire, M. R.; Ogawa, M.; Hama, Y.; Kosaka, N.; Regino, C. A. S.; Choyke, P. L.; Kobayashi, H. *Bioconjugate Chem.* **2008**, *19*, 1735–1742. (h) Johnsson, N.; Johnsson, K. *ACS Chem. Biol.* **2007**, *2*, 31–38. (i) Martí, A. A.; Jockusch, S.; Stevens, N.; Ju, J.; Turro, N. J. *Acc. Chem. Res.* **2007**, *40*, 402–409. (l) Willis, R. C. *Anal. Chem.* **2007**, 1785–1788. (m) Hama, Y.; Urano, Y.; Koyama, Y.; Bernardo, M.; Choyke, P. L.; Kobayashi, H. *Bioconjugate Chem.* **2006**, *17*, 426–1431. (o) Yuste, R. *Nat. Methods* **2005**, *2*, 902–904. (p) Lichtman, J. W.; Fraser, S. E. *Nat. Neuroscience* **2001**, *4*, 1215–1220. (q) Selvin, P. R. *Nat. Struct. Biol.* **2000**, *7*, 730–734.

(2) Lakowicz, J. R. *Principles of Fluorescence Spectroscopy*, 3rd ed.; Springer: New York, 2006.
(3) http://nobelprize.org/nobel_prizes/chemistry/laureates/2008/tsien-lecture.html.
(4) Sullivan, K. F., Ed. *Fluorescent Proteins*, 2nd ed.;Book Series: Methods in Cell Biology; Academic Press, Amsterdam 2008; Vol. 85.
(5) (a) Remington, S. J. *Curr. Opin. Struct. Biol.* **2006**, *16*, 714–721. (b) Ai, H.; Hazelwood, K. L.; Davidson, M. W.; Campbell, R. E. *Nat. Methods* **2008**, *5*, 401–403. (c) Shaner, N. C.; Lin, M. Z.; McKeown, M. R.; Steinbach, P. A.; Hazelwood, K. L.; Davidson, M. W.; Tsien, R. Y. *Nat. Methods* **2008**, *5*, 545–551. (d) Shaner, N. C.; Campbell, R. E.; Steinbach, P. A.; Giepmans, B. N. G.; Palmer, A. E.; Tsien, R. Y. *Nat. Biotechnol.* **2004**, *22*, 1567–1572.

10.1021/ja902416s CCC: $40.75

procedures have been described to make them biocompatible. The development of a sophisticated QD technology has allowed their application to many biological problems, including *in vivo* experiments with NIR fluorescent QDs.[6] QDs have demonstrated superior performance in applications requiring single particle imaging.[6,7] However, there are serious problems with the reproducibility in the quality of biocoated QDs, and reliable tests for the quality of surface coating have not yet been established.[1c] Moreover, the cytotoxicity of QDs in the intracellular metabolism is still a debated question.[8]

Another class of fluorescent dyes that have been extensively studied in the last years is that of conjugated polymer electrolytes for the detection of molecules of biological interest or biologically important ions.[9] Thanks to positively charged pendant groups these polymers can coordinate oppositely charged biological molecules via electrostatic interactions, in particular DNA, while the fluorescence emission of the conjugated backbone is sensitive even to very minor environmental changes. In the presence of polyelectrolytes of biological interest, conjugated polyelectrolytes act as optical transducers of biochemical events by means of changes in fluorescence. Several investigations have concerned the interactions of polythiophene polyelectrolytes with nucleic acids and proteins for the realization of homogeneous biosensors for real-time sequence-specific detection.[9a] Polythiophene electrolytes have also been used for the hystological staining of amyloid deposits in ex vivo tissue samples associated with several pathogenic states.[10] However, the methods based on conjugated polyelectrolytes suffer from the fact that the nature of the complexes they form with biopolymers is poorly known[11] and that in biological fluids other charged macromolecules are generally present besides those of interest, which might contribute to the observed changes in fluorescence.

Molecular fluorescent probes—small organic molecules, the prototype of which is fluorescein isothiocyanate—have been employed for a long time as reporters of events of biological interest.[12] Significant improvements in their optical properties have been achieved over the years. New molecular structures are continuously being engineered.[13] A few families of these compounds—fluorescein and its derivatives and cyanine dyes, in particular—have demonstrated high performance levels in diagnostic applications such as flow cytometry and immunostaining, in the imaging of biological compounds, in DNA labeling, and in FRET experiments.[12] However, molecular fluorescent dyes present limitations in photostability and sensitivity preventing, for example, the long-term imaging of stained and living cells. Having generally narrow bandwidths and small Stokes shifts,[1c] another inconvenience is the limited possibility for multiplexing analysis, which requires irradiation at a single wavelength and the simultaneous observation of the emission of different fluorophores. Nevertheless the appeal of molecular fluorophores lies in the possibility to enhance performance by design and to introduce functional groups that can react with target biocompounds even within living cells. Being small molecules of a few nanometer size, they are ideal candidates to penetrate live cells and illuminate them without altering their metabolism. Owing to the resources of synthetic chemistry, they could in principle be functionalized with almost any functional group and shaped on demand for almost any possible application. In other words, and paraphrasing the title of a well know article from a pioneer in the field of semiconductor oligo and polythiophenes,[14] they are ideal *fluorophores à la carte*, i.e., custom fluorescence dyes to develop and manufacture for the most diverse application areas. However, new systematic studies are needed to renew the toolbox of available molecular fluorophores and push farther their performance. Unquestionably, the better the fluorophores, the easier their manipulation and reproducibility, and the lower their cost, then the better and more numerous the tests are that can be performed.

Owing to the versatile chemistry of thiophene, its easy functionalization, and the fluorescence properties of its oligomers,[15a] we started a few years ago research aimed to explore the possibility of functionalizing these compounds with groups capable of covalently binding relevant biomolecules such as DNA or monoclonal antibodies.[15b−f] These first attempts having been successful, we have now started a more ambitious, wide scope investigation aimed to transform the potentialities into real advantages and original experiments. We wished, on one hand, to control the reactivity of these dyes toward compounds of biological importance by tuning the functionalization of the backbone in view of their use for selective site binding to biocomponents within living cells and, on the other, to enhance and orient their fluorescence properties toward innovative technological applications.

In this paper we report the rapid, efficient, cost-effective, and clean synthesis of a new class of molecular fluorophores more soluble under physiological conditions and more reactivite toward monoclonal antibodies compared to previously described thiophene fluorophores. An easy protocol for multiple labeling of monoclonal antibodies was developed leading also to brightly white emitting antibodies. The use of TFs in immunostaining

(6) (a) Michalet, X.; Pinaud, F. F.; Bentolila, L. A.; Tsay, J. M.; Doose, S.; Li, J. J.; Sundaresan, G.; Wu, A. M.; Gambhir, S. S.; Weiss, S. *Science* **2005**, *307*, 538–544. (b) Gill, R.; Zayats, M.; Willner, I. *Angew. Chem., Int. Ed.* **2008**, *47*, 7602–7625. (c) Medints, I. L.; Tetsuo, H.; Goldman, U. E. R.; Mattoussi, H. *Nat. Mater.* **2005**, *4*, 436–4462. (d) Mahler, B.; Spinicelli, P.; Buil, S.; Quelin, X. *Nat. Mater.* **2008**, *7*, 659–664. (e) Wu, X.; Liu, H.; Liu, J.; Haley, K. N.; Treadway, J. A.; Larson, J. P.; Ge, N.; Peale, F.; Bruchez, M. P. *Nat. Biotechnol.* **2002**, *21*, 41–46.

(7) Temirov, J. P.; Bradbury, A. R. M.; Werner, J. H. *Anal. Chem.* **2008**, *80*, 8642–8648.

(8) (a) Kim, B. Y. S.; Jiang, W.; Oreopoulos, J.; Yip, C. M.; Rutka, J. T.; Chan, W. C. W. *Nano Lett.* **2008**, *8*, 3887–3892. (b) Chang, E.; Thekkek, N.; Yu, W. W.; Colvin, V. L.; Drezek, R. *Small* **2006**, *2*, 1412–1417. (c) Jamieson, T.; Bakhshi, R.; Petrova, D.; Pocock, R.; Imani, M.; Seifalian, A. M. *Biomaterials* **2007**, *28*, 4717–4732.

(9) (a) Ho, H. A.; Najari, A.; Leclerc, M. *Acc. Chem. Res.* **2008**, *41*, 168–178. (b) Herland, A.; Thomsson, D.; Mirzov, O.; Scheblykin, I. G.; Inganäs, O. *J. Mater. Chem.* **2008**, *18*, 126–132. (c) Liu, B.; Bazan, G. C. *Chem. Mater.* **2004**, *16*, 4467–4476. (d) Thomas, S. W., III; Joly, J. D.; Swager, T. M. *Chem. Rev.* **2007**, *107*, 1339–1386.

(10) Nilsson, K. P. R.; Hammarström, P.; Ahlgren, F.; Herland, A.; Schnell, E. A.; Lindgren, M.; Westermark, G. T.; Inganäs, O. *ChemBioChem* **2006**, *7*, 1096–1104.

(11) Chi, C.; Chworos, A.; Zhang, J.; Mikhailovsky, A.; Bazan, G. C. *Adv. Funct. Mater.* **2008**, *18*, 3606–3612.

(12) Haugland, R. P. *A Guide to Fluorescent Probes and Labeling Technologies*; Molecular Probes Inc.: Eugene, OR, 2005.

(13) (a) Özhalici-Ünal, H.; Pow, C. L.; Marks, S. A.; Jesper, L. D.; Silva, G. L.; Shank, N. I.; Jones, E. W.; Burnette, J. M.; Berget, P. B.; Armitage, B. A. *J. Am. Chem. Soc.* **2008**, *130*, 12620–12621. (b) Richard, J. A.; Massonneau, M.; Renard, P. Y.; Romieu, A. *Org. Lett.* **2008**, *10*, 4175–4178. (c) Mottram, L. F.; Boonyarattanakalin, S.; Kovel, R. E.; Peterson, B. R. *Org. Lett.* **2006**, *8*, 581–584. (d) Peneva, K.; Mihov, G.; Herrmann, A.; Zarrabi, N.; Börsch, M.; Duncan, T. M.; Müllen, K. *J. Am. Chem. Soc.* **2008**, *130*, 5398–5399. (e) Kim, D. S.; Ahn, K. H. *J. Org. Chem.* **2008**, *73*, 6831–6834. (f) Umezawa, K.; Nakamura, Y.; Makino, H.; Citterio, D.; Suzuki, K. *J. Am. Chem. Soc.* **2008**, *130*, 1550–1551. (g) Li, L.; Han, J.; Nguyen, B.; Burgess, K. *J. Org. Chem.* **2008**, *73*, 1963–1970.

(14) Garnier, F. *Acc. Chem. Res.* **1999**, *32*, 209–215.

Chart 1. Molecular Structure of Thiophene Fluorophores

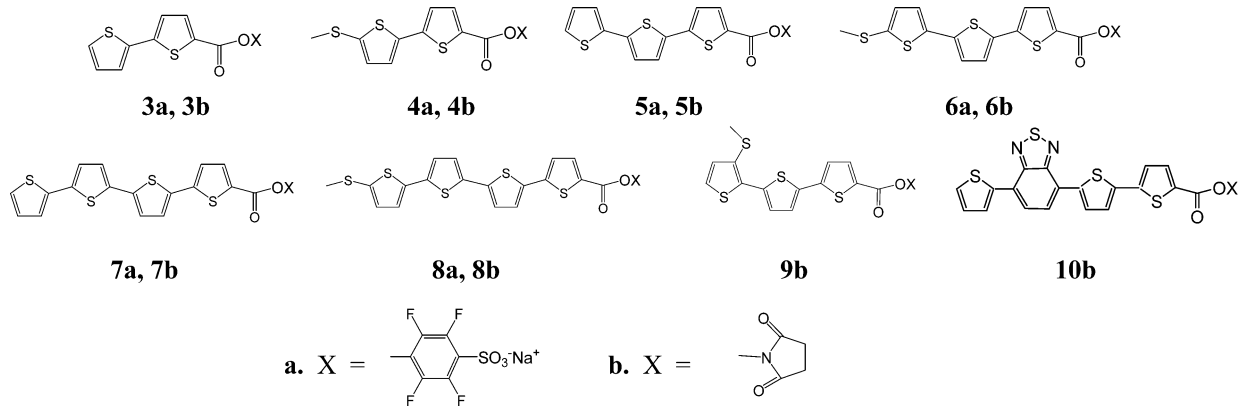

and unprecedented fluorescence stability for this type of experiments are demonstrated. Finally, theoretical calculations furnishing guidelines for further molecular engineering of thiophene based fluorophores are also reported.

2. Experimental Details

2.1. Synthesis. The synthesis of compounds **2**−**8**, their characterization, and the materials used for their preparation are described in detail in the Supporting Information (pages S1−S15).

2.2. Optical Characterization. Absorption and photoluminescence spectra were obtained using a Perkin-Elmer Lamda 20 spectrophotometer and a Perkin-Elmer LS50B spectrofluorometer, respectively. For all dyes photoluminescence was recorded exciting at the maximum wavelength absorption. Solvents were spectral grade. Details of quantum yield measurements and other additional information are reported as Supporting Information (pages S20−S22).

2.3. Computational Details. All theoretical calculations were performed using the TURBOMOLE 5.9 program package.[16] Ground state and excited state geometries were fully optimized employing the B3-LYP[17,18] hybrid density functional and triple-ζ basis set with polarization functions on all atoms (TZVP).[19] Dipole moments were obtained from the Kohn−Sham densities for the ground state and from the excited-state relaxed density for the excited state.[20] More details are given in the Supporting Information (page S18).

2.4. Labeling and Multiple Labeling of Monoclonal Antibodies (MoAbs). MoAb anti-CD38 was furnished by Professor Fabio Malavasi, Laboratory of Immunogenetics, Department of Genetics, Biology and Biochemistry, University of Torino Medical School, Torino, Italy. MoAb anti-CD4 was furnished by Beckman Coulter, Miami, USA. The detailed procedure for conjugation of the fluorophores to the antibodies is described in Supporting Information (pages S19−S22). The fluorophore to protein molar ratio was estimated spectrophotometrically according to standard procedures.[21]

2.5. Immunostaining Experiments. Lymphocytes from an MOLT-4 cell line were employed. The cell staining protocol is described in detail in the Supporting Information (pages S24−S26).

A fluorescence microscope (Olympus, Model BX52) equipped with a halogen lamp (100 W) for transmitted light, 100 W HBO (mercury) lamp for fluorescence, and mirror units for ultraviolet, violet, blue violet, and blue excitation was employed to observe fluorescence emissions of MOLT-4 cells stained with different MoAbs labeled with TFs.

3. Results and Discussion

Two classes of thiophene based fluorophores (TFs) have already been described: isothiocyanates (TF-NCS) and *N*-hydroxysuccinimidyl esters (TF-NHS). To improve solubility in aqueous media and employ more effective synthetic protocols, we have now developed a third class of TFs, namely thiophene based 4-sulfo-2,3,5,6-tetrafluorophenyl esters (TF-STP). The molecular structures of TFs-STP and TFs-NHS analyzed in this study are shown in Chart 1.

3.1. Synthesis of Thiophene Based 4-Sulfo-2,3,5,6-tetrafluorophenyl Esters (TFs-STP). Tetrafluoro-phenyl esters of bi-, ter-, and quaterthiophene (compounds **3a**−**8a**) are described for the first time. The detailed synthesis and ^{1}H, ^{13}C, and ^{19}F NMR spectra are reported as Supporting Information (pages S9−S16).

Compared to *N*-hydroxysuccinimidyl esters (**3b**−**8b**) synthesized by conventional methodologies,[15b,c,e] TFs-STP **3a**−**8a** were obtained much more rapidly and in higher yields by taking advantage of microwave irradiation.[22] The synthetic strategy is illustrated in Scheme 1. It consists of building up the aromatic skeleton by sequential Pd(II) catalyzed Suzuki cross couplings of newly synthesized or commercial borylated and halogenated building blocks with the final addition of thienyl tetrafluorosulphonate (**2**) prepared starting from commercial 5-bromo-2-thiophenecarboxylic acid (**1**). The coupling of **2** to boronic esters to obtain the desired TF-STP was complete after only 2 min of microwave irradiation. Due to the hydrophilic character of TFs-STP, aqueous workup was avoided.

A rapid and high-yield purification by chromatography on florisil removed the excess of boronic ester and the base used.

(15) (a) Barbarella, G.; Melucci, M.; Sotgiu, G. *Adv. Mater.* **2005**, *17*, 1581–1593. (b) Barbarella, G.; Zambianchi, M.; Pudova, O.; Paladini, V.; Ventola, A.; Cipriani, F.; Gigli, G.; Cingolani, R.; Citro, G. *J. Am. Chem. Soc.* **2001**, *123*, 11600–11607. (c) Barbarella, G.; Zambianchi, M.; Ventola, A.; Fabiano, E.; Della Sala, F.; Gigli, G.; Anni, M.; Bolognesi, A.; Polito, L.; Naldi, M.; Capobianco, M. *Bioconjugate Chem.* **2006**, *17*, 58–67. (d) Zambianchi, M.; Barbieri, A.; Ventola, A.; Favaretto, L.; Bettini, C.; Galeotti, M.; Barbarella, G. *Bioconjugate Chem.* **2007**, *18*, 1004–1009. (e) Capobianco, M. L.; Cazzato, A.; Alesi, S.; Barbarella, G. *Bioconjugate Chem.* **2008**, *19*, 171–177. (f) Quarta, A.; Di Corato, R.; Manna, L.; Argentiere, S.; Cingolani, R.; Barbarella, G.; Pellegrino, T. *J. Am. Chem. Soc.* **2008**, *130*, 10545–10555. (g) Piacenza, M.; Zambianchi, M.; Barbarella, G.; Gigli, G.; Della Sala, F. *Phys. Chem. Chem. Phys.* **2008**, *10*, 5363–5373.
(16) Ahlrichs, R, et al. Universität Karlsruhe2007. See also: http://www.turbomole.com.
(17) Becke, A. D. *J. Chem. Phys.* **1993**, *98*, 5648–5652.
(18) Lee, C.; Yang, W.; Parr, R. G. *Phys. Rev. B* **1988**, *37*, 785–789.
(19) Schäfer, A.; Huber, C.; Ahlrichs, R. *J. Chem. Phys.* **1994**, *100*, 5829–5835.
(20) Furche, F.; Ahlrichs, R. *J. Chem. Phys.* **2002**, *117*, 7433–7447.
(21) Brinkley, M. *Bioconjugate Chem.* **1992**, *3*, 2–13.
(22) (a) Polshettiwar, V.; Varma, R. S. *Chem. Soc. Rev.* **2008**, *37*, 1546–1557. (b) Alesi, A.; Di Maria, F.; Melucci, M.; Macquarrie, D. J.; Luqueb, R.; Barbarella, G. *Green Chem.* **2008**, *10*, 517–523. (c) Melucci, M.; Barbarella, G.; Zambianchi, M.; Di Pietro, P.; Bongini, A. *J. Org. Chem.* **2004**, *69*, 4821–4828.

Scheme 1. Synthetic Pattern for the Preparation of TFs-STP[a]

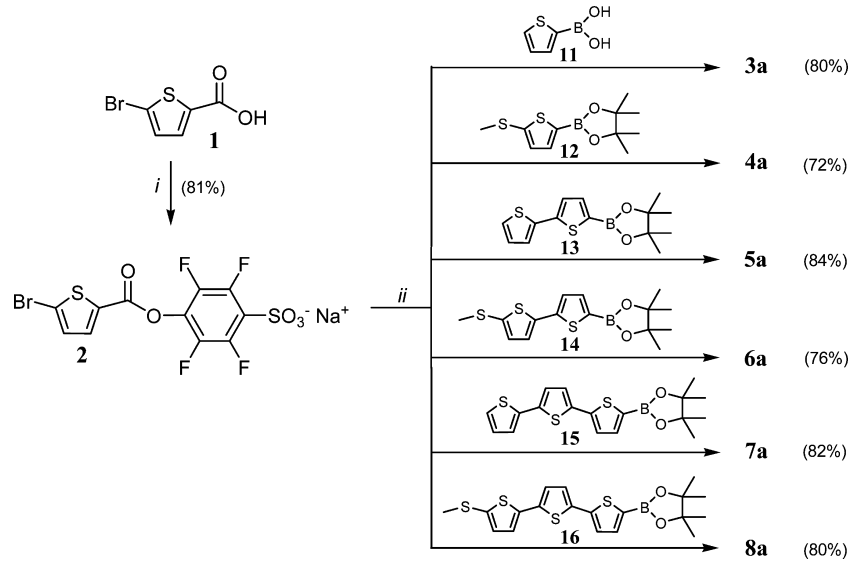

[a] Reagents and conditions: (*i*) 4-sulfotetrafluorophenol, sodium salt, DCC, acetone/DMF 15:1, rt, 16 h; (*ii*) $NaHCO_3$, $PdCl_2$dppp, DMF/H_2O 9:1, μv 2 min, 80 °C. Yields in isolated product in parentheses.

This simple protocol leads to very rapid reaction times, is environmentally friendly and cost-effective, and allows easy tuning of the molecular structure, hence of the optical properties, by changing the size and the substituents of the aromatic backbone prior to the addition of thienyl tetrafluorosulphonate.

The use of microwaves prevents the formation of undesired products arising from the occurrence of boron−halogen exchange, a slower reaction compared to cross coupling, allowing a dramatic simplification of the purification procedures of the crude reaction products. The synthesis could be scaled up to 300 mg at a time. The synthetic details, in particular the synthesis of methylthio-thienyl, -bithienyl, and -terthienyl boronic acid pinacol esters, are reported as Supporting Information (pages S2−S8).

3.2. Optical Properties and Theoretical Calculations. The absorption and emission spectra of oligothiophene 4-sulfo-2,3,5,6,-tetrafluorophenyl esters **3a**−**8a** measured in DMSO are shown in Figure 1, whereas those of compounds **3b**−**10b** have already been reported.[15c,e] Table 1 gives the absorption and emission wavelengths and the molar absorption coefficients of **3a,b-8a,b** in DMSO.

The spectral characteristics of TFs-STP are similar to those of the corresponding TFs-NHS, and band shapes and bandwidths (60−120 nm) are essentially the same for both classes of fluorophores, which is not surprising since the fluorophores have the same emitting aromatic component and only differ in the nature of the amine-reactive substituent. All compounds are characterized by large Stokes shifts from absorption to emission, much greater than those of common molecular fluorophores.[1c] While the absorption wavelengths vary in the range 350−450 nm, the emission wavelengths are spread from 450 to 650 nm, spanning almost over the entire visible range.

The most important property of TFs is their photostability. No matter what the functional group is, -NCS, -NHS or -STP, the fluorophores can be excited continuously for hours without loosing their brightness. As powders, in air, they are stable for years. In solution, the esters may slightly be hydrolyzed while only the fluorescence frequency, but not the intensity, is modified from that of an ester to that of the corresponding acid. An experiment comparing the photostability of **6a** in solution with

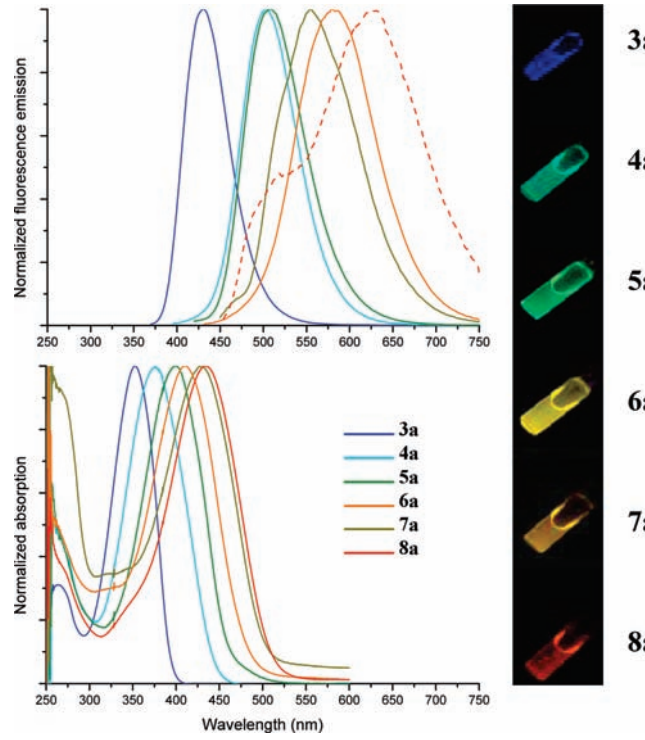

Figure 1. Normalized absorption and fluorescence emission spectra of compounds **3a**−**8a** in DMSO and palette of the fluorescence colors. The PL spectra were obtained by irradiating each compound at the maximum wavelength absorption. The photograph shows the fluorescence emission of all compounds under irradiation at $\lambda_{exc} = 364$ nm with a 15 W UV lamp.

that of fluorescein under irradiation with a 100 W mercury lamp is reported as Supporting Information (page S21).

Table 1 reports the fluorescence quantum yield of compounds **3a**−**7a** and **3b**−**7b** measured in dimethylsulfoxide. The quantum yields of compounds **9b** and **10b** (Chart 1) in the same solvent are 0.42 and 0.34, respectively.

Table 1 shows that the quantum yields are very similar for NHS and STP esters, not unexpectedly considering that the two

Table 1. Absorption (λ_{max}, nm) and Emission (λ_{PL}, nm) Wavelengths, Molar Absorption Coefficients (ϵ, M^{-1} cm^{-1}), and Fluorescence Quantum Yields (ϕ)[a] of **3a,b**−**8a,b** 10^{-5} M in DMSO

item	λ_{max}	ϵ	λ_{PL}	ϕ	item	λ_{max}	ϵ	λ_{PL}	ϕ
3a	353	23.200	430	0.78	**4a**	376	19.900	503	0.70
3b	350	22.600	430	0.71	**4b**	380	22.700	500	0.74[b]
5a	400	24.100	508	0.27	**6a**	410	21.100	580	0.35
5b	400	34.400	507	0.42	**6b**	412	28.600	580	0.37[b]
7a	429	31.900	555	0.26	**8a**	434	34.300	515, 625[c]	0.26
7b	430	25.600	565	0.31	**8b**	438	39.000	625	0.31

[a] Estimated error: ±0.05. [b] 1.00 ± 0.05 and 0.76 ± 0.05 for **4b** and **6b**, respectively, in CH_2Cl_2. From ref 15d. [c] DMSO/H_2O 90:10.

types of fluorophores have the same emitting components. Interestingly, for NHS as well as for STP esters, ϕ decreases on increasing the size of the fluorophore, from the >0.7 value of the bithiophene esters to the ∼0.3 value of the quaterthiophene esters. Both the quantum yield values and the trend of variation with size are remarkably different from those of the corresponding unsubstituted bi-, ter-, and quaterthiophene (quantum yield ranging from ∼0.02 for bithiophene to ∼0.06 for terthiophene and ∼ 0.2 for quaterthiophene).[23] The reasons for such behavior have not yet been elucidated and require much deeper photophysical study.

We noticed that for all esters the fluorescence efficiency was drastically reduced on passing from DMSO to a H_2O buffered solution, probably due to aggregation phenomena since we also observed that the decrease was progressively attenuated on decreasing the concentration of the solution. Judging from the intensity of the corresponding PL spectra, the fluorescence efficiency increased again when the fluorophore in a buffered solution was reacted with the antibody, probably because in the bioconjugate the fluorophores are well separated from each other. Using commercial molecular dyes, we obtained similar results, but we were unable to find accurate investigations on this point. Thus, we are currently carrying out a comparative study on this important point.

As a result of increasing the number of thiophene rings, or introducing a SCH_3 substituent, the photoluminescence shifts toward longer wavelengths. The SCH_3 substituent is an electron donor, while the carbonyl group at the opposite end of the molecule is an electron acceptor; hence the fluorophore is a "push−pull" compound with an increased π-electron delocalization. In compound **9b**, where the SCH_3 group is in the β-position, the electron donor effect of the substituent is partially counteracted by increased molecular distortion due its steric effects.[24] As a consequence, the shift from absorption to emission for **9b** is smaller than that for **6b**. The photoluminescence of these "push−pull" fluorophores is very sensitive to environment changes, as shown in Figures 23S, 24S and Table 1S reporting the changes in λ_{PL} observed on varying the solvent. Figure 2 compares the changes in photoluminescence wavelength observed on going from toluene (with a dielectric constant of 2.4) to DMSO (with a dielectric constant of 48.9) for a dimer-NHS (**4b**, λ_{PL} from 458 to 502 nm), a linear trimer-NHS (**6b**, λ_{PL} from 509 to 582 nm), a linear trimer-STP (**6a**, λ_{PL} from 519 to 580 nm), and a branched trimer-NHS (**9b**, λ_{PL} from 489 to 539 nm). On increasing the dielectric constant value, a progressive displacement toward longer wavelengths is observed.

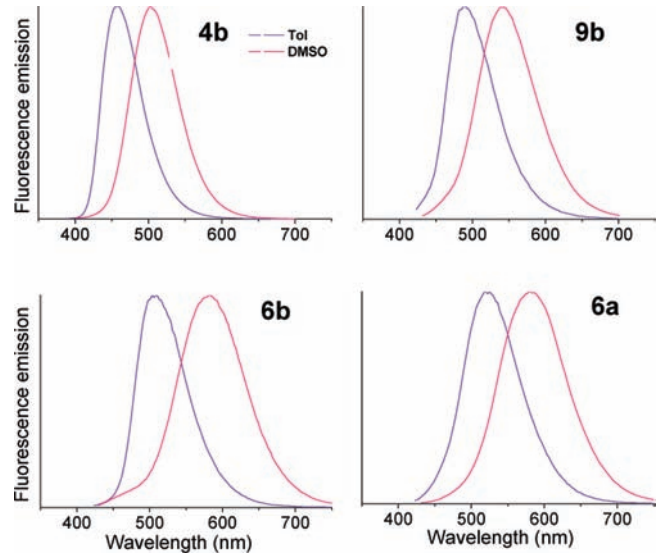

Figure 2. Normalized fluorescence emission spectra of compounds **4b**, **9b**, **6b**, and **6a** in toluene (blue line) and in DMSO (red line), obtained by exciting each compound at the maximum wavelength absorption.

Table 2. TD-DFT Calculated Absorption (E_{ABS}) and Emission (E_{PL}) Energies[a], Molecular Dipole Moments in the Ground (μ_g) and Excited State (μ_e)[b] and Experimental and Theoretical Emission Peak Shifts[c] from Toluene to DMSO

	E_{ABS}	E_{PL}	μ_g	μ_e	ΔE_{exp}	ΔE_{theor}
4b	3.41 (363)	2.82 (439)	1.7992	7.7835	0.24	0.26
6b	2.94 (421)	2.49 (497)	2.7927	10.4534	0.24	0.24
9b	2.94 (421)	2.44 (507)	1.5725	10.9622	0.31	0.30

[a] In eV (nm in brackets). [b] In debye. [c] In eV.

The observed effect only concerns the excited states since the corresponding absorption spectra (Figure 23S) are insensitive to solvent changes. Note that the fluorescence emission wavelengths of unsubstituted thiophene oligomers do not vary with the solvent.[23]

To shed light on the solvent effect observed on the photoluminescence of "push−pull" TFs, we have carried out first-principles TD-DFT theoretical calculations in the homogeneous series of *N*-succinimidyl esters **4b**, **9b**, and **6b**, where the electron donor substituent is either α or β to sulfur. The corresponding computed excitation and emission energies are reported in Table 2, while Figure 3 shows the optimized molecular structure and molecular electrostatic potential of the fluorophores in the ground state (left) and excited state (right), together with the direction and size of the molecular dipole moments.

All transitions can be traced back to strongly dipole allowed excitations from the highest occupied (HOMO) to the lowest unoccupied (LUMO) molecular orbital. The calculated values of absorption and photoluminescence energies agree very well (i.e., within the accuracy of the method) with the experimental results.

The absorption energy of dimer **4b** is calculated at 3.41 eV (363 nm) and the emission energy at 2.82 eV (439 nm), which corresponds to a large Stokes shift of 0.59 eV. For trimers **9b** and **6b** TD-DFT computed energies are equivalent in absorption, whereas the emission energy of **9b** is slightly red-shifted with respect to that of **6b**, as found experimentally. The resulting

(23) Becker, R. S.; Seixas de Melo, J.; Macüanita, A. L.; Elisei, F. *J. Phys. Chem.* **1996**, *100*, 18683–18695.
(24) Barbarella, G.; Zambianchi, M.; Antolini, L.; Folli, U.; Goldoni, F.; Iarossi, D.; Schenetti, L.; Bongini, A. *J. Chem. Soc. Perkin Trans. 2* **1995**, 1869–1873.

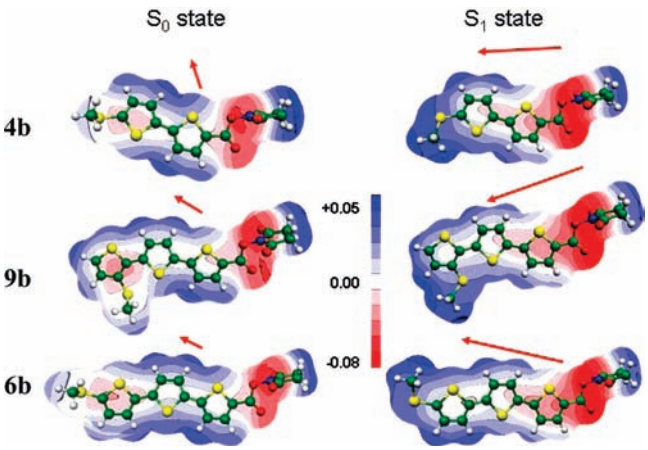

Figure 3. Optimized molecular structure and molecular electrostatic potential in the ground state (left) and excited state (right) for compounds **4b**, **9b**, and **6b**. The direction and size of the molecular dipole moments are reported as red arrows.

Stokes shifts are 0.45 and 0.50 eV for **9b** and **6b**, respectively. Comparison of the values for **4b** and **6b** shows that the increase in conjugation length leads to a red shift in absorption of 0.47 eV and in emission of 0.27 eV, whereas the different positions of the SCH_3 substituent in **9b** and **6b** have a much smaller impact.

Table 2 also reports the dipole moments in the ground state (μ_g) and in the first optically allowed excited state (μ_e), which are also shown in Figure 3 together with the molecular electrostatic potential. Dipole moments are much larger than those previously reported for unsubstituted *N*-succinimidyl bithiophenes,[15g] due to the presence of the SCH_3 group.

The ground state dipole moments of **4b**, **9b**, and **6b** have different intensities and directions due to a complex interplay of the charges localized on SCH_3 and on the succinimidyl groups. In the excited state, on the other hand, the calculations predict a strong increase of the molecular dipole moment, which arises from an accumulation of negative charge on the succinimidyl group and of positive charge on the methyl group of the methylsulfinyl substituent. In contrast to **4b** and **6b**, in **9b** the dipole moment in the ground and excited state are almost parallel owing to the reduced molecular size caused by the different position of the SCH_3 substituent. In addition, the changes in the molecular geometries induced by electronic excitation contribute to a change in the dipole moment, as shown in Figure 3 where the optimized molecular geometries in the ground and excited states are reported. In the ground state geometry, the thiophene rings are in the anti orientation. The corresponding dihedral angles are found in the range 158°−164°, and the methylsulfanyl group adopts an approximately perpendicular orientation with respect to the neighboring thiophene ring. In the first excited state, the bithiophene and terthiophene cores planarize and the SCH_3 substituent rotates until the previously perpendicular dihedral angle is reduced to 45° for TF **4b**, 36° for **9b**, and 29° for **6b**.

The dipole moments in the ground and excited states were used to compute the photoluminescence energy ($E^{PL}_{solv.}$) as a function of the dielectric constant of the solvent according to the Amos−Burrows equation (see Supporting Information, p S18). In the last two columns of Table 2 the experimental and calculated photoluminescence energy differences from toluene to dimethylsulfoxide ($\Delta E = E^{PL}_{tol} - E^{PL}_{DMSO}$) are compared. The agreement between theory and experiment is very good, and more importantly, it clearly reflects an increased solvent effect for dye **6b** due to the much larger dipole changes in the excited state. Thus, **6b** should present red-shifted emission in high-dielectric constant environments.

The calculation results, in agreement with experimental data, indicate that the insertion of electron-donor substituents of different "push" strength in different positions of the aromatic backbone is a way to achieve fine-tuning of the fluorescence emission and to realize fluorescent probes that are fine reporters of environment changes.

3.3. Labeling and Multiple Labeling of Monoclonal Antibodies. The labeling of antibodies with fluorescent dyes, namely immunofluorescence, is widely used in different fields such as medical diagnostics, molecular biology, or environmental monitoring, owing to the high specificity and versatility of immunoassays.[12]

Dyes **3**−**10** are amine reactive compounds and can be covalenty bound to monoclonal antibodies (MoAbs) through reaction of the X = NHS or STP functional groups with the NH_2 groups of ϵ-lysine residues of MoAb under basic conditions.[12,15c]

$$\text{Biopolymer}-NH_2 + \text{TF}-C(O)-OX \rightarrow \text{Biopolymer}-NH-C(O)-\text{TF}$$

3.3.1. Labeling Experiments with TFs. Both classes of fluorophores, TFs-NHS and TFs-STP, were reacted with the anti-CD38 monoclonal antibody in the same experimental conditions to allow the comparison of the fluororophore to protein (F/P) molar ratios achieved for the same aromatic moiety but different functional group. Anti-CD38 is a human monoclonal antibody directed against the cell surface glycoprotein CD-38 present on various immune cells and with potential antineoplastic activity.[25,26] In the Experimental Details we report the protocol used to bind **3a,b**−**8a,b** with anti-CD38. The reaction time was arbitarily fixed at 30 min.

Figure 4 shows the absorption and emission spectra of the anti-CD38 MoAb labeled with TFs-STP and TFs-NHS.

Table 3 reports the absorption and emission wavelengths of anti-CD38 MoAbs measured in PBS buffer pH = 7.4, together with the fluorophore to protein molar ratios, F/P, estimated from the relative intensities of protein and dye absorptions.[21,15d] In the table the absorption signal arising from the protein, ∼280 nm in all cases, is omitted.

The F/P values achieved in 30 min with TFs-STP are generally higher than those achieved with the corresponding TFs-NHS, indicating a greater reactivity of the -STP with respect to the -NHS functional group, the lowest F/P ratios having been obtained with quaterthiophene derivatives.

The insertion of an SCH_3 group causes a marked red shift in the antibody emission wavelength for dimers and trimers but not for tetramers, as already observed for the free fluorophores. For MoAbs labeled with dimers and trimers, the emission

(25) (a) Deaglio, S.; Mallone, R.; Baj, G.; Donati, D.; Giraudo, G.; Corno, F.; Bruzzone, S.; Geuna, M.; Ausiello, C.; Malavasi, F. *FASEB J.* **2001**, *15*, 580–582. (b) Alessio, M.; Roggero, S.; Funaro, A.; De Monte, L.B.,; Peruzzi, L.; Geuna, M.; Malavasi, F. *J. Immunol.* **1990**, *145*, 878–3884. Patten, P. E. M.; Buggins, A. G. S.; Richards, J.; Wotherspoon, A.; Salisbury, J.; Mufti, G. J.; Hamblin, T. J.; Devereux, S. *Blood* **2008**, *111*, 5173–5181.

(26) (a) Zhu, S.; Zhang, Q.; Guo, L. H. *Anal. Chim. Acta* **2008**, *624*, 141–146. (b) Zhang, Q.; Guo, L. H. *Bioconj. Chem* **2007**, *18*, 1668–1672. (c) Luchowski, R.; Matveeva, E. G.; Gryczynski, I.; Terpetschnig, E. A.; Patsenker, L.; Laczko, G.; Borejdo, J.; Gryczynski, Z. *Curr. Pharm. Biotechnol.* **2008**, *9*, 411–420.

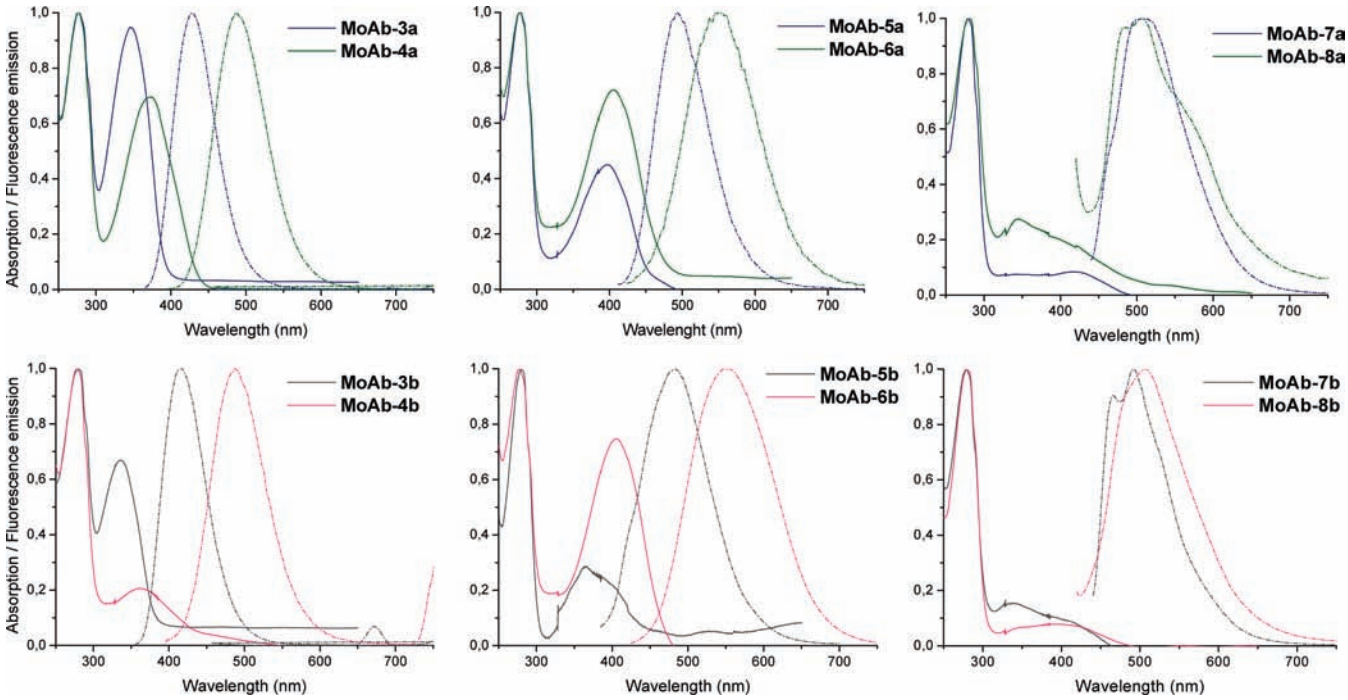

Figure 4. Normalized absorption and fluorescence emission spectra of anti-CD38 monoclonal antibody (MoAb) labeled with TFs-STP (**3a**−**8a**) and TFs-NHS (**3b**−**8b**) fluorophores (incubation time: 30 min).

Table 3. Absorption (λ_{max}, nm) and Emission (λ_{PL}, nm) Wavelengths of Anti-CD38 Monoclonal Antibodies Labeled with Fluorophores **3a,b**−**8a,b** in PBS Buffer pH = 7.4 and Fluorophore to Protein Molar Ratios (F/P)

item	λ_{max}	λ_{PL}	*F/P*	item	λ_{max}	λ_{PL}	*F/P*
MoAb-3a	346	427	11	**MoAb-4a**	370	487	8
MoAb-3b	336	415	8	**MoAb-4b**	365	488	2
MoAb-5a	395	492	5	**MoAb-6a**	405	550	12
MoAb-5b	365	480	2	**MoAb-6b**	405	550	11
MoAb-7a	420	520	1	**MoAb-8a**	420	500, 580	3
MoAb-7b	420	465, 490	1	**MoAb-8b**	420	510	1

bandwidth is remarkably sharper for TFs-STP compared to the corresponding TFs-NHS. We temptatively assume that this is the result of the greater reactivity of TFs-STP allowing the binding of all fluorophores to the same site of the antibody, an interpretation which also explains the differences in absorption and emission between the two classes of compounds reported in Table 3.

In all cases a blue shift is observed for both the absorption and emission signals compared to those of the free fluorophores (Table 1), but the Stokes shifts from absorption to emission remain quite large.

The labeled antibodies are highly stable, chemically as well optically. We have now been keeping labeled antibodies (anti-CD4, anti-CD3 from different sources and anti-CD38) for years at 4 °C and verified their unaltered biological activity and fluorescence properties. More detailed information on this point and the comparison with the same antibodies labeled with commercial molecular fluorophores will be reported in a separate paper.

3.3.2. Multiple-Labeling Experiments with TFs and White Emitting Antibodies. Multiple labeling of antibodies is starting to be investigated in fluorescence immunoassays to implement new labeling strategies to meet the demand for high sensitivity in the detection of molecules of biological interest[25a,b] or in single molecule studies for the understanding of the behavior of complex biomolecules in real time.[25]

The easy manipulation of thiophene fluorophores and their photostability allowed us to perform facile multiple labeling of monoclonal antibodies with TFs. Here we report experiments carried out using the same antibody (anti-CD4 or anti-CD38 MoAbs) simultaneously labeled with different TFs, excited using one single light source and resulting in intense white light emission.

At the beginning, our intention was, on one hand, to verify the possibility to create new color shades by mixing TFs of different colors as we had already realized with oligothiophene thin films[27] and, on the other, to explore the possibility of FRET (Fluorescence Resonance Energy Transfer)[2] to enhance the intensity of the red emitters through irradiation of appropriate blue emitters with much higher fluorescence efficiencies. For fluorescence resonance energy transfer to be observed, the excited fluorophore must emit at a wavelength matching the absorption wavelength of the second fluorophore and the two fluorophores must be located in close proximity (generally 5−6 nm).[2,28]

Since we had control of the choice of the fluorophores but not of the position at which they would be attached in the antibody, we reasoned that with the lack of FRET we could verify the occurrence of multiple labeling by choosing complementary emission colors, blue and orange, in particular, and observe whether there was white light emission from the antibody. The protocol used for the multilabeling experiments is reported in detail in the Supporting Information.

(27) Anni, M.; Gigli, G.; Paladini, V.; Cingolani, R.; Barbarella, G.; Favaretto, L.; Sotgiu, G.; Zambianchi, M. *Appl. Phys. Lett.* **2000**, *77*, 2458–2460.
(28) Kozlov, V. G.; Bulovic, V.; Burrows, P. E.; Baldo, M.; Khalfin, V. B.; Parthasarathy, G.,; Forrest, S. R. *J. Appl. Phys.* **1998**, *84*, 4096–4108.

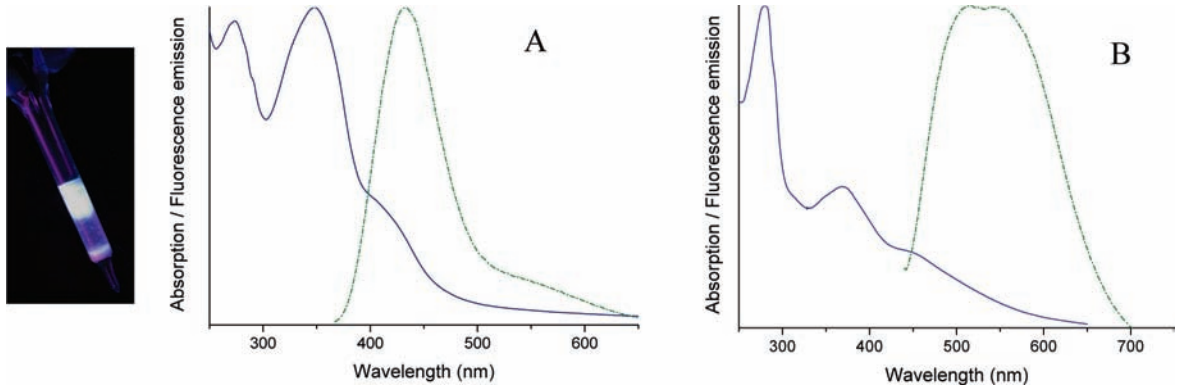

Figure 5. Normalized absorption and emission spectra of white fluorescent anti-CD38 and anti-CD4 monoclonal antibodies, labeled with compounds **3a/6a** and **4b/10b**, respectively. The fluorescence spectra were obtained by exciting the samples with $\lambda_{exc} = 347$ and 420 nm, respectively. The photograph is that of the anti-CD38 antibody within a Sephadex column under irradiation with a 15 W UV lamp at $\lambda_{exc} = 364$ nm.

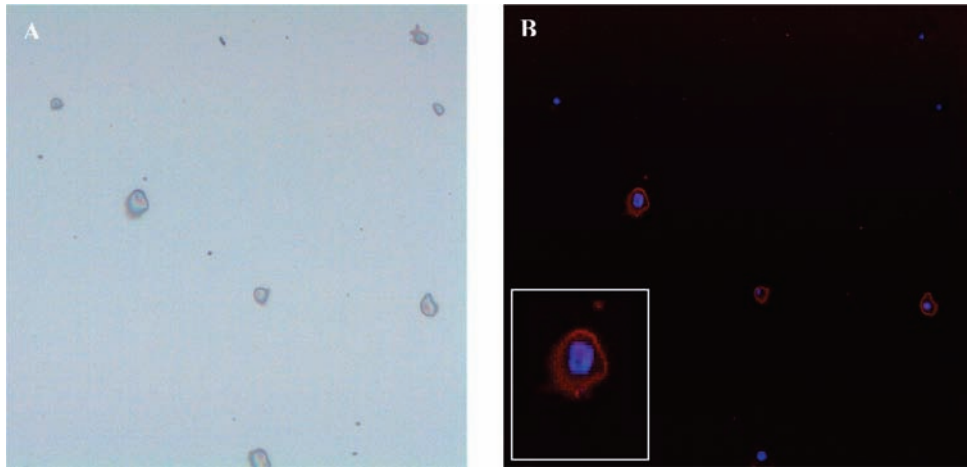

Figure 6. Fluorescence microscopy images (× 20) of human T lymphocytes (MOLT-4 cell line) stained using the anti-CD4 monoclonal antibody labeled with fluorophore **6b**. (A) Light transmission image. (B) Fluorescence microscopy image after staining with **6b** and counterstaining with DAPI. The inset shows the magnified image of one of the cells.

Despite the large choice of fluorophores allowed by the TFs available to us, and the use of two different antibodies (anti-CD4 and anti-CD38), we did not observe any fluorescence transfer energy from blue to red. We did instead observe the occurrence of white fluorescence upon excitation with one single light source. Thus, the relative amounts of blue and orange fluorophores were accurately weighed to obtain intense and neat white emission from the antibody (see the Supporting Information).

Figure 5A shows the absorption spectrum of the anti-CD38 MoAb labeled with both **3a** and **6a** and the corresponding emission spectrum obtained by irradiating at $\lambda_{exc} = 347$ nm. At this wavelength both dyes are simultaneously excited. By irradiating with a 15 W UV lamp at $\lambda_{exc} = 364$ nm, it was possible to observe with the naked eye the intense white fluorescence of the antibody within a Sephadex column.

The frequency of the single light excitation source could be finely tuned toward longer wavelengths by choosing the appropriate fluorophores. Figure 5B shows the absorption and emission spectra of the anti-CD4 monoclonal antibody labeled with fluorophores **4b** and **10b**. The optical characteristics of **10b** ($\lambda_{max} = 470$ nm, $\lambda_{PL} = 590$ nm in CH_2Cl_2, and $\lambda_{PL} = 615$ nm in DMSO) are described in the Supporting Information and in ref 15f. In this case simultaneous excitation of the blue and red emitting fluorophore was obtained by exciting at $\lambda_{exc} = 420$ nm. A further example is reported in the Supporting Information (p S21).

From these results we conclude that the fluorophore binding sites in the MoAb are too distant to allow the energy transfer to occur from the blue to the orange emitter. Nevertheless, to our surprise, we obtained experimental evidence that energy transfer does occur when the multiple-labeled MoAb is fixed on the cell membrane in immunostaining experiments. This is difficult to assess quantitatively, and we are currently trying to put our initial observations on a more solid basis. Also difficult to quantify is the gain in fluorescence intensity associated with multiple labeling compared to the monolabeling of a given antibody. In principle, the more photons are absorbed, the more intense the fluorescence signal is, and indeed qualitatively the signal arising from antibodies labeled with multiple TFs is very intense and bright. However, again, a methodology to ensure signal quantification and reproducibility has still to be developed. What at the moment is clear is that the procedure described above to immobilize multiple fluorophores on a single antibody is very simple to implement and is worthy of further study.

3.4. Immunostaining Experiments with TFs. The labeling of antibodies with fluorescent dyes may be used to visualize the subcellular distribution of biomolecules of interest. For example, a primary monoclonal antibody such as anti-CD4 may be used

to specifically recognize and bind the corresponding antigen protein located on the cell membrane (immunostaining). If the antibody is labeled with a fluorescent dye, analysis with a fluorescence microscope indicates the location of the antigen. Immunostaining experiments require a meticulous setup, from cells preparation and fixation to fluorescence microscopy analysis, to optimize the signal arising from the antibody bound to the corresponding antigen on the cell membrane.

We have developed a protocol for the staining of fixed cells with TFs which is reported in detail in the Supporting Information (pp S24−S26). In Figure 6 we show the immunostaining of the MOLT 4 cell line (T lymphocytes) with the anti-CD4 MoAb labeled with fluorophore **6b**.

Cells are a very complex environment which is difficult to mimic in vitro. The cellular environment of our samples under the experimental conditions employed for staining was such that **6b** was intensely orange-red fluorescent, as predicted by theoretical calculations (see above) in environments with a high dielectric constant.

Figure 6B shows the orange-red fluorescence emission of the cell membrane of the lymphocytes stained with the anti-CD4/**6b** conjugate and counterstained with DAPI, namely 4′,6-diamidino-2-phenylindole, a blue emitting dye which colors selectively the nucleus of fixed cells.[2] Normally, the antigen on the cell surface is present only on a fraction of the cells. Anti-CD4 is a Mouse IgG2 isotype monoclonal antibody reacting with CD4, a 55 kDa molecular weight glycoprotein expressed on the cell surface of nearly 60% of peripheral blood T lymphocytes. In agreement with this, in Figure 6B only a portion of the cells display orange-red staining of the cell membrane while all cells display the blue staining of the nucleus due to DAPI. Figure 6B shows great morphological detail and the fine intense orange-red fluorescence of the cell membrane well separated from the fluorescence of the nucleus.

Loss of fluorescence caused by photobleaching (conversion of a fluorophore into a nonfluorescent state by the absorbed photons) is the source of many problems in immunostaining experiments, mainly due to the need for reduced times for light excitation exposure. Time course examination of our samples showed that after 3 h from the first observation with repeating light exposure the emission signal had not changed and was still intensely bright. During the 3 h time course, with the slides being exposed to microscope light continuously for 5 min each 10 min for a total of 12 times, we did not observe any change in the fluorescence image. The same slides of Figure 6B, kept in air into a clean room at 18−22 °C without any light protection, were observed 1 and 3 months after immunostaining (see Figure 23SA and 23SB of the Supporting Information). The quenching of the blue fluorescence of DAPI was observed, while there was only a slight loss of the orange-red fluorescence due to **6b**. Further examples of fixed cell staining will be reported in a separate paper.

4. Conclusions

Molecular fluorophores stand out from the many classes of available fluorescent dyes because they can easily be built up *via* organic synthesis to meet the growing demand of tailor-made tools for biomolecular detection, sensing, and multiplexing analysis.

The results reported here indicate that thiophene based molecular fluorophores, TFs, can be tailored to satisfy the conditions for a wide range of applications requiring highly stable and long lasting fluorescence emission, facile emission tunability through appropriate substitution, and multilabeling experiments employing a single light excitation source. A desired functional group can be added to a preselected emitting core employing standard modalities to increase hydrophilicity and reactivity, to optimize photophysical properties and/or the specific linkage to target biomolecules. Belonging to the same chemical family, TFs can easily be combined for multicolor applications in bioresearch. For all these aspects, thiophene fluorophores are true "*fluorophores à la carte*".

One of the most interesting achievements realized with TFs is their outstanding optical stability allowing a significant extension of fluorescence observation times with respect to currently employed dyes. Monoclonal antibodies labeled and multilabeled with TFs are brightly fluorescent and can undergo repeated excitation cycles without any fluorescence loss. In immunostaining experiments using TFs, unaltered fluorescence emission was observed from the cells for at least 3 weeks and repeated exposition to laser excitation. These results show that TFs are highly suitable for analyses by fluorescence microscopy in clinical diagnostics, and laboratory research and pave the way to applications in cytofluorimetry, in which cells are immunostained in solution.

We are currently working to the realization of a set of thiophene fluorophores for spontaneous uptake by live cells which are also functionalized to target specific cell components.

Acknowledgment. F.D.S. and M.P. acknowledge support from the ERC-Starting Grant FP7-Project DEDOM (no. 207441). This work was partially supported by the project SYNERGY (FIRB RBNE03S7XZ_005). We are grateful to Prof. Fabio Malavasi, University of Torino and to Beckman Coulter, Miami, USA, for the generous gifts of anti-CD38 and anti-CD4 monoclonal antibodies. Thanks are also due to Laura Favaretto and Cristian Bettini (CNR-ISOF Bologna, Italy) and to Dr. Alfredo Ventola (INFM-CNR, Lecce) for expert technical assistance. We are also grateful to Dr. Andrea Barbieri (CNR-ISOF Bologna, Italy) for help with fluorescence quantum yield measurements.

Supporting Information Available: Detailed synthesis, NMR spectra and mass spectra of **3a**−**8a**; details of optical properties and theoretical calculations; detailed procedures for labeling and multiple labeling of monoclonal antibodies; detailed procedures for immunostaining. This material is available free of charge via the Internet at http://pubs.acs.org.

JA902416S